Bioorganic & Medicinal Chemistry Letters 21 (2011) 2969–2974

Contents lists available at ScienceDirect

Bioorganic & Medicinal Chemistry Letters

journal homepage: www.elsevier.com/locate/bmcl

NMS-P937, a 4,5-dihydro-1*H*-pyrazolo[4,3-*h*]quinazoline derivative as potent and selective Polo-like kinase 1 inhibitor

Italo Beria [a,*], Roberto T. Bossi [a], Maria Gabriella Brasca [a], Michele Caruso [a], Walter Ceccarelli [a], Gabriele Fachin [a], Marina Fasolini [a], Barbara Forte [a], Francesco Fiorentini [b], Enrico Pesenti [a], Daniele Pezzetta [b], Helena Posteri [a], Alessandra Scolaro [a], Stefania Re Depaolini [a], Barbara Valsasina [a]

[a] *Nerviano Medical Sciences srl, Business Unit Oncology, Viale Pasteur 10, 20014 Nerviano, MI, Italy*
[b] *Accelera srl, Viale Pasteur 10, 20014 Nerviano, MI, Italy*

ARTICLE INFO

Article history:
Received 21 February 2011
Revised 14 March 2011
Accepted 14 March 2011
Available online 21 March 2011

Keywords:
PLK1
Polo-like kinase
Kinase inhibitor
In vivo activity
Phase I clinical trials

ABSTRACT

As part of our drug discovery effort, we identified and developed 4,5-dihydro-1*H*-pyrazolo[4,3-*h*]quinazoline derivatives as PLK1 inhibitors. We now report the optimization of this class that led to the identification of NMS-P937, a potent, selective and orally available PLK1 inhibitor. Also, in order to understand the source of PLK1 selectivity, we determined the crystal structure of PLK1 with NMS-P937. The compound was active in vivo in HCT116 xenograft model after oral administration and is presently in Phase I clinical trials evaluation.

Antimitotics form the basis of the therapy for patients with both solid tumors and hematological malignancies. However, current antimitotic drugs affect both dividing and non-dividing cells. One of the emerging next generation antimitotic targets is Polo-like kinase 1 (PLK1).[1] Among the four members of PLK family, PLK1 is the best characterized and it is recognized to be a key component of the cell cycle control machinery with important roles in the mitotic entry, centrosome duplication, bipolar mitotic spindle formation, transition from metaphase to anaphase, cytokinesis and maintenance of genomic stability.[2–5] PLK1 is often over-expressed in many different tumor types and over-expression often correlates with poor prognosis.[6,7] As an antimitotic target, PLK1 is only expressed in dividing cells while it is not expressed in differentiated postmitotic cells like neurons, where instead expression of PLK2 and PLK3 was reported. This indicates a potentially better safety profile for a PLK1 specific inhibitor.[1,8] Thus, PLK1 is thought to be a promising target for anti-cancer therapy and indeed some PLK1 inhibitors are currently under evaluation in clinical trials.[9]

In the recent past we have identified the 4,5-dihydro-1*H*-pyrazolo[4,3-*h*]quinazoline template as a good scaffold to obtain potent and selective PLK1 inhibitors **1** and **2** (Fig. 1).[10,11] Subsequently work continued on the class in order to discover a specific and orally available PLK1 inhibitor that is suitable for clinical trials. Efforts to improve the solubility and pharmacokinetic profile of lead compound **2** by a focused expansion at the 5′- and 1-positions of the 4,5-dihydro-1*H*-pyrazolo[4,3-*h*]quinazoline scaffold led to the identification of a new potent, selective and orally bioavailable inhibitor.

Compounds modified at the 5′-position, were prepared by reacting the iodo amide **3** with the suitable anilines **4a–f** and $Pd(OAc)_2$ under Buchwald–Hartwig conditions, to obtain final compounds **5a–b** and intermediates **5c–f** (Scheme 1).[12] Intermediates **5e–f** were then converted to final compounds **5g–h**, by removal of the benzyl protecting group with BCl_3. Reaction of bromo intermediate **5c** with the suitable primary or secondary amines under Buchwald–Hartwig conditions, catalyzed by $Pd_2(dba)_3$ and 2-dicyclohexylphosphino-2′-(*N*,*N*-dimethylamino)-biphenyl, gave compounds **5i–l** and the protected intermediate **5m** that was converted to the final compound **5n** by treatment with 4 M HCl (Scheme 2). Synthesis of

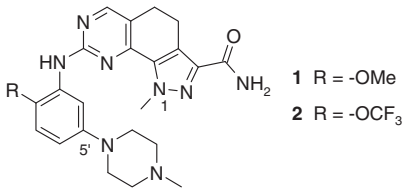

Figure 1. Structure of PLK1 inhibitors **1** and **2**.

* Corresponding author. Tel.: +39 331 581516; fax: +39 331 581347.
E-mail address: italo.beria@nervianoms.com (I. Beria).

0960-894X/$ - see front matter © 2011 Elsevier Ltd. All rights reserved.
doi:10.1016/j.bmcl.2011.03.054

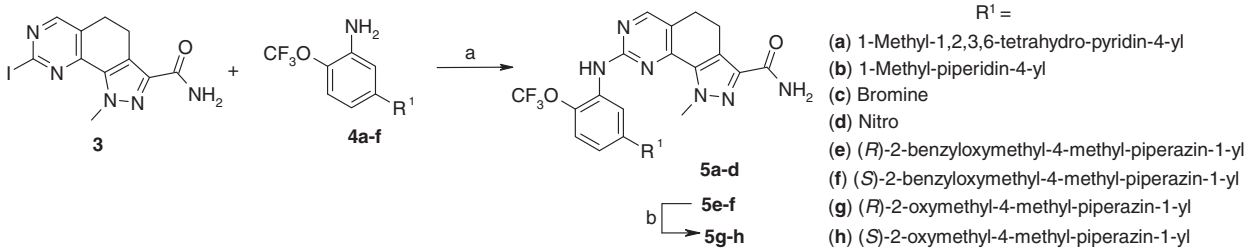

Scheme 1. Reagents and conditions: (a) $Pd(OAc)_2$, (±)-BINAP, K_2CO_3, anilines **4a**–**f**, DMF, 80 °C, 20–62%; (b) under nitrogen atmosphere, BCl_3, DCM, −78 °C then rt, 12 h, quantitative.

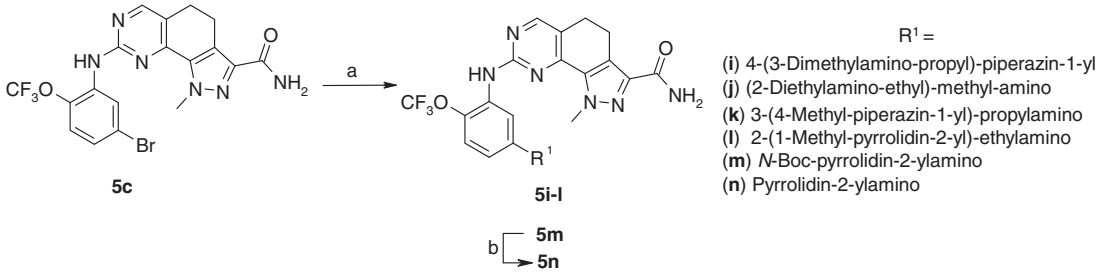

Scheme 2. Reagents and conditions: (a) primary or secondary amines, $Pd_2(dba)_3$, 2-dicyclohexylphosphino-2′-(*N*,*N*-dimethylamino)-biphenyl, $LiN(TMS)_2$, THF, reflux, 10–70%; (b) 4 M HCl in dioxane, dioxane, rt, quantitative.

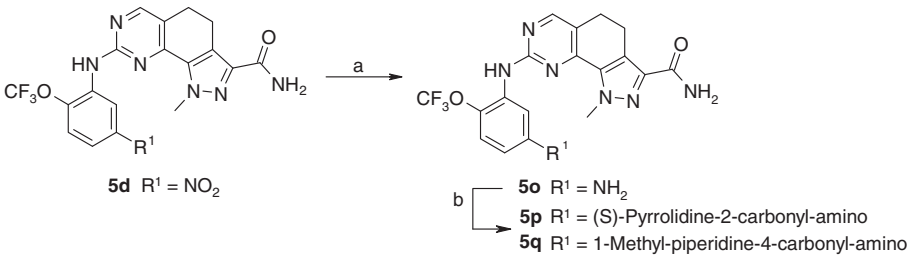

Scheme 3. Reagents and conditions: (a) Fe, NH_4Cl, MeOH/H_2O, reflux, quant.; (b) *O*-(benzotriazol-1-yl)-*N*,*N*,*N*′,*N*′-tetramethyluronium tetrafluoroborate (TBTU), HOBt, DIPEA, acids, 4 h, rt, 60%, then to yield **5p** DCM, TFA, rt, 30 min, 30% (2 steps).

derivatives **5p**–**q** were carried out by reducing the nitro intermediate **5d** to the amino derivative **5o** with Fe and NH_4Cl then, coupling **5o** with suitable acids in the presence of *O*-(benzotriazol-1-yl)-*N*,*N*,*N*′,*N*′-tetramethyluronium tetrafluoroborate (TBTU) as a condensing agent to directly yield the final derivative **5q** or, in two steps, after removal of the BOC protecting group, the compound **5p** (Scheme 3). Modifications at the 1-position of the 4,5-dihydro-1*H*-pyrazolo[4,3-*h*]quinazoline nucleus, to install the piperazino residue were performed reacting the advanced intermediate **6**[12] with 4-methyl-piperazine under Buchwald–Hartwig conditions, then selective alkylation at the 1-position of the pyrazolo ring with alkyl halogens under basic conditions, yielded, either directly or through removal of the protecting group, the final compounds **7a** and **7e**–**g** (Scheme 4).[12]

Table 1 summarizes the structure–activity relationship (SAR) of derivatives modified at the 5′-position of the hit compound **2**. All the compounds, with the exception of **5o** and **5p**–**q**, showed an increased solubility with respect to the hit **2**. The compounds wherein the 1-methyl piperazin-4-yl appendix has been replaced with either 1-methyl-1,2,3,6-tetrahydro-pyridine-4-yl (**5a**) or with

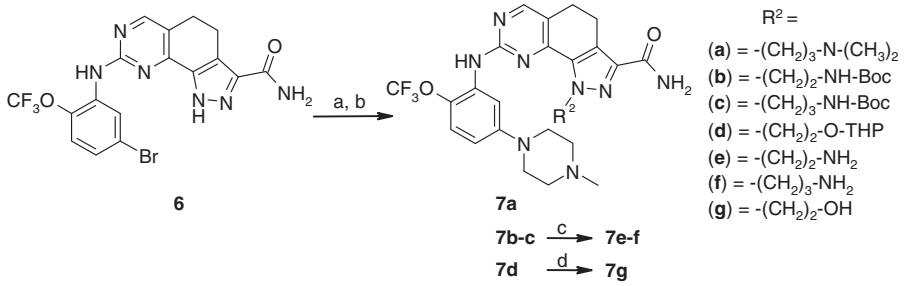

Scheme 4. Reagents and conditions: (a) 4-methyl-piperazine, $Pd_2(dba)_3$, 2-dicyclohexylphosphino-2′-(*N*,*N*-dimethylamino)-biphenyl, $LiN(TMS)_2$, THF, reflux, 70%; (b) Cs_2CO_3, R^2-Cl or R^2-Br, DMF, rt, 20–60%; (c) 4 N HCl in dioxane, rt, 4 h, quant.; (d) TsOH, EtOH, rt, 60%.

Table 1
SAR: variation at the 5′-position of the aniline residue

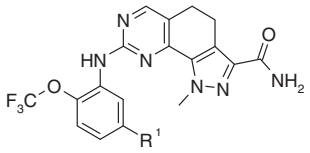

Compound	R^1	PLK1 IC_{50}[a] (μM)	PLK2 IC_{50}[a] (μM)	PLK3 IC_{50}[a] (μM)	A2780 IC_{50}[a] (μM)	Solubility pH 7 (μM)
2	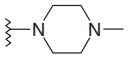	0.003 ± 0.001	3.519 ± 0.063	1.439 ± 0.078	0.021 ± 0.005	72
5a	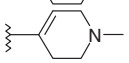	0.003 ± 0.001	2.254 ± 0.77	0.323 ± 0.062	0.034 ± 0.006	148
5b	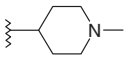	0.006 ± 0.003	>10	>10	0.090 ± 0.002	203
5i	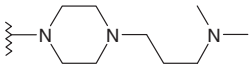	0.042 ± 0.010	3.855 ± 0.467	1.315 ± 0.182	0.526 ± 0.041	174
5p	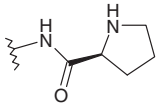	0.044 ± 0.011	1.453 ± 0.106	0.681 ± 0.219	0.348 ± 0.008	79
5j	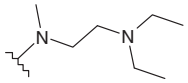	0.060 ± 0.028	>10	>10	1.136 ± 0.077	162
5n	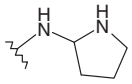	0.083 ± 0.021	0.762 ± 0.034	0.239 ± 0.008	2.209 ± 0.296	171
5o	NH_2	0.087 ± 0.033	1.280 ± 0.464	0.154 ± 0.024	1.074 ± 0.123	31
5k	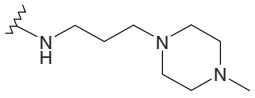	0.106 ± 0.044	1.364 ± 0.341	0.713 ± 0.064	1.635 ± 0.416	186
5l	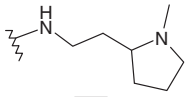	0.149 ± 0.051	0.429 ± 0.017	0.485 ± 0.046	2.549 ± 0.411	157
5g	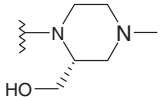	0.154 ± 0.032	>10	>10	0.598 ± 0.186	121
5h	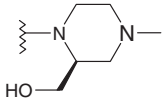	0.201 ± 0.012	1.494 ± 0.211	3.519 ± 0.708	1.615 ± 0.475	166
5q	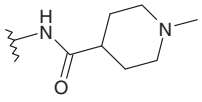	0.224 ± 0.043	1.499 ± 0.337	0.705 ± 0.073	1.353 ± 0.180	33

[a] Values are means of three experiments. Compounds **5c** and **5d** showed PLK1 IC_{50} >1 μM and were not further profiled.

1-methyl piperidin-4-yl (**5b**) residues maintain the PLK1 activity, the selectivity profile versus PLK2–3 and the antiproliferative effect on A2780 cells line of the hit **2**. The other compounds, although more soluble than **2**, showed from 14-fold (**5i**) to 74-fold (**5q**) decreased PLK1 activity and a more drastic reduction of the cytotoxic activity on cells, ranging from 15-fold (**5p**) to more than 120-fold (**5l**).

Activity data concerning compounds modified at position 1 of the pyrazole ring of the hit compound **2** are summarized in Table 2. Although replacement of methyl residue with either primary (**7e** and **7f**) or tertiary (**7a**) amines increases the solubility of the compounds it also led to a reduction of potency in both the biochemical and cellular assays. In particular, the best compound **7e** showed a 10-fold loss of activity on PLK1 and a more than 50-fold decreased cytotoxicity in A2780 cell lines. This heavy loss in cell activity, shared also by the other amine derivatives **7a** and **7f**, could be explained with a decreased ability of the molecules to enter into the cells, due to their higher hydrophilicity, as confirmed by in vitro permeability data. For example, the hit compound **2** resulted indeed to be highly permeable ($P_{app} = 50 \times 10^{-6}$ cm/s), while compounds **7e–f** resulted to be low/medium permeable ($P_{app} = 5 \times 10^{-6}$ cm/s and 4×10^{-6} cm/s, respectively).[13] Replacement of the methyl residue with the 2-hydroxyethyl residue (**7g**) resulted instead very profitable. Actually, compound **7g** showed the same activity of hit **2**, both in the biochemical assay and in cells. Moreover, it exhibited an increased solubility and an improved selectivity for PLK1 with respect to the other two isoforms PLK2-3, and also on a larger kinases panel, where at least 300-fold selectivity was found.[14]

The most promising compounds **5a**, **5b** and **7g** were further evaluated in vitro for ADME properties and data were compared with those of hit **2** (Table 3). Among the three players, compound

Table 2
SAR: variation at the 1-position of the pyrazole ring

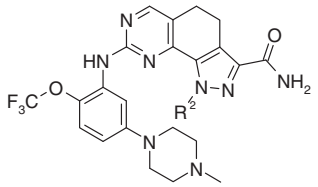

Compound	R^2	PLK1 IC_{50}[a] (μM)	PLK2 IC_{50}[a] (μM)	PLK3 IC_{50}[a] (μM)	A2780 IC_{50}[a] (μM)	Solubility pH 7 (μM)
7g	$-(CH_2)_2-OH$	0.002 ± 0.001	>10	>10	0.042 ± 0.007	201
2	$-CH_3$	0.003 ± 0.001	3.519 ± 0.063	1.439 ± 0.078	0.021 ± 0.005	72
7e	$-(CH_2)_2-NH_2$	0.033 ± 0.012	>10	>10	1.307 ± 0.388	202
7d	$-(CH_2)_2-O-THP$	0.043 ± 0.003	>10	1.002 ± 0.264	0.126 ± 0.027	35
7f	$-(CH_2)_3-NH_2$	0.052 ± 0.021	>10	>10	0.846 ± 0.186	186
7a	$-(CH_2)_3-N-(CH_3)_2$	0.279[b]	>10	>10	2.501[b]	200

[a] Values are means of three experiments.
[b] Single data.

Table 3
In vitro ADME[a] properties of selected compounds

Compound	Solubility 10% Tween 80 (mg/mL)	Permeability Caco-2[b] (P_{app})	PAMPA[c] (P_{app} 10^{-6} cm/s)	Cl_{int} (mL/min/kg) rat hepatocytes (1 μM)	Cl_{int} (mL/min/kg) HLM[d] (1 μM)
2	>3.2	High	50.00	600 ± 15	25.70 ± 0.20
5a	3.7	Moderate	46.41	638 ± 21	24.50 ± 0.31
5b	3.8	High	36.78	603 ± 12	15.95 ± 0.06
7g	>3.4	Moderate	49.59	165 ± 7	16.90 ± 0.15

[a] Absorption, distribution, metabolism and excretion.
[b] Permeability class has been ascribed using Ranitidine and *N*-acetyl-DL-phenylalaninamide as low or high permeable reference compounds, respectively.
[c] Parallel artificial membrane permeability assay.
[d] Human liver microsomes.

Table 4
In vivo pharmacokinetic parameters[a] ±standard deviation of selected compounds in CD1 nu/nu mice[b]

Compound	PK data (iv), dose[c]: 10 mg/kg				PK data (po), dose[c]: 10 mg/kg			
	AUC_∞ (μM h)	CL (L/h/kg)	V_{ss} (L/kg)	$t_{1/2}$ (h)	C_{max} (μM)	AUC_∞ (μM h)	$t_{1/2}$ (h)	F[d] (%)
2	4.97 ± 0.71	4.21 ± 0.45	3.39 ± 0.03	0.92 ± 0.12	0.29 ± 0.04	1.04 ± 0.10	1.44 ± 0.29	21
7g	8.57 ± 1.18	2.36 ± 0..33	1.71 ± 0.11	0.89 ± 0.01	0.64 ± 0.24	2.04 ± 0.50	1.60 ± 0.57	24

[a] Data of compounds **2** and **7** were compared statistically using Student's *t*-test; P <1% for CL and V_{ss}, P = 1.1% for AUC_∞ and P >5% for $t_{1/2}$ after iv administration were found; P = 2.5% for AUC_∞, and P >5% for C_{max} and $t_{1/2}$ after oral administration were calculated.
[b] n = 3 animals per study.
[c] Dosed as HCl in situ salt/glucosate.
[d] Bioavailability.

Table 5
In vivo intravenous activity of compounds **2** and **7g** on HCT116 tumor in nude mice[a]

Compound	Treatment	Dose (mg/kg)	$\%TGI_{max}$ (day)	$\%BWL_{max}$ (day)
2	1–2 bid × 3 weekly cycles	30	81 (32)	14 (30)
7g	1–3 bid × 2 weekly cycles	45	83 (24)	16 (15)

[a] n = 7 animals per study.

7g came out as the best, showing similar permeability, in both Caco-2 and PAMPA assay, with respect to **5a** and **5b** but higher metabolic stability in rat hepatocytes (Cl_{int} = 165 vs 638 and 603 mL/min/Kg, respectively). In view of its better overall profile, compound **7g** was selected for further evaluation. In vivo pharmacokinetic properties of **7g** were evaluated in Harlan nu/nu mice, following intravenous (iv) and oral (po) dosing and data were compared with those of compound **2** (Table 4).[11,15] Compound **7g** showed a pharmacokinetic profile slightly better than **2** with higher AUC and C_{max}, lower clearance, and acceptable oral bioavailability (F = 24%).

The mechanism of action of compound **7g** was evaluated in different cell lines by fluorescent activated cell sorting (FACS), western blot and immunocytochemical analysis and in analogy to 5-dihydro-1*H*-pyrazolo[4,3-*h*]quinazoline analogs,[10,11] resulted in agreement with PLK1 inhibition (Valsasina et al., manuscript in preparation).

Efficacy of **7g** was evaluated in vivo in CD1 nu/nu mice xenografted with human HCT116 colon adenocarcinoma cells. The compound **7g** when administered intravenously (iv) at 45 mg/kg, bid at days 1, 2, 3, in a weekly scheduling × 2 cycles, showed a good tumor growth inhibition (TGI_{max} = 83%, day 24) with acceptable and

Table 6
In vivo oral activity of compounds **2** and **7g** on HCT116 tumor in nude mice[a,b]

Compound	Dose (mg/kg)	%TGI$_{max}$ (day)	%BWL$_{max}$ (day)	Death
2	90	59 (18)	14 (15)	3
7g	90	71 (36)	10 (36)	0
	120	84 (36)	18 (29)	0

[a] $n = 7$ animals per study.
[b] 1–2 daily × 4 weekly cycles treatment.

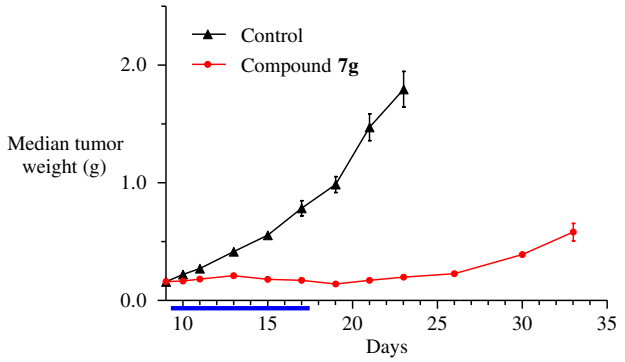

Figure 2. In vivo oral antitumor activity of **7g** at 60 mg/kg, once a day, 1–10 consecutive days (blue line) on HCT116 xenograft model.

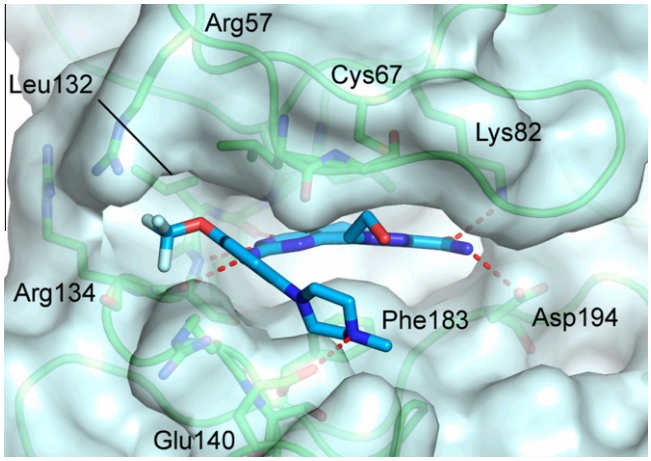

Figure 3. Compound **7g** bound to PLK1. Hydrogen bonds are shown as red dashed lines.

reversible body weight loss (BWL$_{max}$ = 16%, day 15) (Table 5). Higher activity and better tolerability was shown by compound **7g**, with respect to **2**, after oral administration (po) (Table 6). When given orally at 90 mg/kg, once a day at days 1, 2, in a weekly scheduling × 4 cycles, compound **2** showed low activity (TGI$_{max}$ = 59%) with 3/7 death. At the same dose and scheduling, compound **7g** exhibited good activity (TGI$_{max}$ = 71%, day 36) without any death. In addition, the dose could be increased to 120 mg/kg, without death and with an improvement of activity (TGI$_{max}$ = 84%, day 36). The better safety profile of **7g** in comparison with **2** was reaffirmed in the 1–10 daily oral scheduling treatment, where partial regression on 6/7 animals was obtained at 60 mg/kg with TGI$_{max}$ = 89% at day 23 (Fig. 2). At the same daily dose of **7g** (60 mg/kg), compound **2** showed toxicity with 5 out of 7 death at five days after the end of the treatment. In view of its better selectivity and safety profile, together with its suitability for a more flexible scheduling, compound **7g** (NMS-P937) was selected for in vivo activity on additional tumor models and for toxicological studies that led to its selection as clinical candidate.

The 2.2 Å crystal structure of the PLK1 kinase domain (residues 36–345) in complex with NMS-P937 was solved to fully characterize the interactions between the enzyme and inhibitor and to better understand the source of the PLK1 selectivity.[16] As expected, NMS-P937 binds in the ATP-pocket and most of the interactions are similar to those found in the past with a close analog.[10] Specifically, NMS-P937 makes a series of donor–acceptor–donor hydrogen bonds with the PLK1 hinge residues (Glu131 & Cys133) and the amide moiety hydrogen bonds with Lys82 and Asp194 (Fig. 3). The pyrazolo-quinazoline core of NMS-P937 is sandwiched between Cys67 and Phe183 and the attached ethyl hydroxyl extends into the ribose pocket. The 2′-trifluoromethoxy group binds in a pocket formed by Arg57 and the hinge segment Leu132-Cys133-Arg134 and multipolar interactions are present between fluorine atoms and the guanidinium group of Arg57 and the backbone carbonyl of Arg134. Presumably, the 'fit' of the 2′-trifluoromethoxy group in this pocket plays a crucial role in obtaining PLK selectivity versus kinases bearing a residue bulkier in the position corresponding to Leu132, such as those present in Aurora-A and CDK2. In addition, the 5′-methylpiperazine moiety contributes to the PLK1 selectivity with respect to PLK 2–3 since it establishes a polar interaction with the side chain of Glu140 and the same type of interaction is hampered in both PLK2 and PLK3 where Glu140 is replaced by histidine.[10,17]

In summary, we report the identification of NMS-P937, a new PLK1 specific inhibitor that was found to be highly potent on the target and highly selective versus PLK2 and PLK3 isoforms, as well as in a wide kinase panel. The compound showed good solubility and PK properties suitable for either iv or oral administration. When tested in vivo by oral administration, NMS-P937 showed good activity and good tolerability also after prolonged treatment. For its favorable characteristics, NMS-P937 was selected for clinical development. NMS-P937 is the first selective PLK1 inhibitor given orally to enter Phase I clinical studies.

Acknowledgments

We thank the group of Assay Development and Biochemical Screening for the biochemical assay on kinase panel, Dario Ballinari and the group of Cell Screening for cell proliferation assay, Paolo Cappella for FACS analysis, Jay Bertrand for crystal structure and discussion, Daniele Donati and Eduard R. Felder for their useful comments on the manuscript.

Supplementary data

Supplementary data (mechanism of action by FACS analysis and kinase profile of compound **7g**) associated with this article can be found, in the online version, at doi:10.1016/j.bmcl.2011.03.054.

References

1. Strebhardt, K. *Nat. Rev. Drug Disc.* **2010**, *9*, 643.
2. Garland, L. L.; Taylor, C.; Pilkington, D. L.; Cohen, J. L.; Von Hoff, D. D. *Clin. Cancer Res.* **2006**, *12*, 5182.
3. Santamaria, A.; Neef, R.; Eberspaecher, U.; Eis, K.; Husemann, M.; Mumberg, D.; Prechtl, S.; Schulze, V.; Siemeister, G.; Wortmann, L.; Barr, F. A.; Nigg, E. A. *Mol. Biol. Cell* **2007**, *18*, 4024.
4. Barr, F. A.; Sillje, H. H.; Nigg, E. A. *Nat. Rev. Mol. Cell Biol.* **2004**, *5*, 429.
5. van Vugt, M. A.; van de Weerdt, B. C.; Vader, G.; Janssen, H.; Calafat, J.; Klompmaker, R.; Wolthuis, R. M.; Medema, R. H. *J. Biol. Chem.* **2004**, *279*, 36841.
6. Weichert, W.; Schmidt, M.; Gekeler, V.; Denkert, C.; Stephan, C.; Jung, K.; Loening, S.; Dietel, M.; Kristiansen, G. *Prostate* **2004**, *60*, 240.
7. Weichert, W.; Kristiansen, G.; Winzer, K. J.; Schmidt, M.; Gekeler, V.; Noske, A.; Muller, B. M.; Niesporek, S.; Dietel, M.; Denkert, C. *Virchows Arch.* **2005**, *446*, 442.

8. Kauselmann, G.; Weiler, M.; Wulff, P.; Jessberger, S.; Konietzko, U.; Scafidi, J.; Staubli, U.; Bereiter-Hahn, J.; Strebhardt, K.; Kuhl, D. *EMBO J.* **1999**, *18*, 5528.
9. Schoffski, P. *Oncologist* **2009**, *14*, 559.
10. Beria, I.; Ballinari, D.; Bertrand, J. A.; Borghi, D.; Bossi, R. T.; Brasca, M. G.; Cappella, P.; Caruso, M.; Ceccarelli, W.; Ciavolella, A.; Cristiani, C.; Croci, V.; De Ponti, A.; Fachin, G.; Ferguson, R. D.; Lansen, J.; Moll, J. K.; Pesenti, E.; Posteri, H.; Perego, R.; Rocchetti, M.; Storici, P.; Volpi, D.; Valsasina, B. *J. Med. Chem.* **2010**, *53*, 3532.
11. Beria, I.; Valsasina, B.; Brasca, M. G.; Ceccarelli, W.; Colombo, M.; Cribioli, S.; Fachin, G.; Ferguson, R. D.; Fiorentini, F.; Gianellini, L. M.; Giorgini, M. L.; Moll, J. K.; Posteri, H.; Pezzetta, D.; Roletto, F.; Sola, F.; Tesei, D.; Caruso, M. *Bioorg. Med. Chem. Lett.* **2010**, *20*, 6489.
12. Caruso, M.; Beria, I.; Brasca, M. G.; Ferguson, R.; Posteri, H.; Valsasina, B. Patent WO 2008074788, 2008.
13. Kansy, M.; Senner, F.; Gubernator, K. *J. Med. Chem.* **1998**, *41*, 1007.
14. The panel includes c-ABL, AKT1, Aur-A, Aur-B, BRK, BUB1, CDC7, CDK1/B, CDK2/A, CDK2/E, CDK4/D1, CDK5/P25, CHK1, CK2, EEF2K, EGFR1, EphA2, ERK2, FAK, FGFR1, FLT3, GSK3β, Haspin, IGFR1, IKK2, IR, JAK1, JAK3, KIT, LCK, LYN, MAP-KAPK2, MELK, MET, MNK2, MPS1, MST4, NEK6, NIM, P38α, PAK4, PDGFR, PDK1, PERK, PIM1, PIM2, PKAα, PKCβ, RET, ROS1, SULU1, SYK, TLK2, TRKA, TYK2, VEGFR2, VEGFR3 and ZAP70.
15. The pharmacokinetic profiles of the compounds were investigated in overnight fasted male nu/nu mice following a single dose given intravenously (iv) or orally (po). Blood samples of each mouse were taken from saphenous vein at different time and after centrifugation plasma samples were analyzed by LC/MS/MS technique. For a more complete description see Ref. 10.
16. Coordinates of the PLK1 complex with compound **7g** have been deposited in the Protein Data Base under accession code 2YAC, together with the corresponding structure factor file.
17. Emmitte, K. A.; Adjebang, G. M.; Andrews, C. W.; Badiang Alberti, J. G.; Bambal, R.; Chamberlain, S. D.; Davis-Ward, R. G.; Dickson, H. D.; Hassler, D. F.; Hornberger, K. R.; Jackson, J. R.; Kuntz, K. W.; Lansing, T. J.; Mook, R. A., Jr.; Nailor, K. E.; Pobanz, M. A.; Smith, S. C.; Sung, C.; Cheung, M. *Bioorg. Med. Chem. Lett.* **2009**, *19*, 1694.